Chemical Science

ROYAL SOCIETY OF CHEMISTRY

EDGE ARTICLE

View Article Online
View Journal | View Issue

Cite this: *Chem. Sci.*, 2024, **15**, 14977

All publication charges for this article have been paid for by the Royal Society of Chemistry

The backbone constitution drives passive permeability independent of side chains in depsipeptide and peptide macrocycles inspired by *ent*-verticilide†

Madelaine P. Thorpe, [a] Abigail N. Smith, [a] Daniel J. Blackwell, [b] Corey R. Hopkins, [c] Bjorn C. Knollmann, [b] Wendell S. Akers[d] and Jeffrey N. Johnston *[a]

The number of peptide-like scaffolds found in late-stage drug development is increasing, but a critical unanswered question in the field is whether substituents (side chains) or the backbone drive passive permeability. The backbone is scrutinized in this study. Five series of macrocyclic peptidic compounds were prepared, and their passive permeability was determined (PAMPA, Caco-2), to delineate structure–permeability relationships. Each series was based on the cell-permeable antiarrhythmic compound *ent*-verticilide, a cyclic oligomeric depsipeptide (COD) containing repeating ester/*N*-Me amide didepsipeptide monomers. One key finding is that native lipophilic ester functionality can impart a favorable level of permeability, but ester content alone is not the final determinant – the analog with highest P_{app} was discovered by a single ester-to-*N*-H amide replacement. Furthermore, the relative composition of esters and *N*-Me amides in a series had more nuanced permeability behavior. Overall, a systematic approach to structure–permeability correlations suggests that a combinatorial-like investigation of functionality in peptidic or peptide-like compounds could better identify leads with optimal passive permeability, perhaps prior to modification of side chains.

Received 25th April 2024
Accepted 9th August 2024

DOI: 10.1039/d4sc02758b

rsc.li/chemical-science

Introduction

Recent breakthroughs in the translation of bioactive peptide hits to successful marketed drugs[1] has changed the perception of viable chemotypes for drug development.[2,3] While the enhancement of binding remains the critical effort to achieve maximal potency and selectivity *in vitro*, a peptidic screening hit[4] must also be endowed with cell membrane permeability[5,6] when targeting intracellular receptors.[7] Polar functional groups, including amide and ester, play a key role in conformation, metabolism, and permeability. However, the design principles for interconversion of these functional groups to manipulate permeability are largely undeveloped.

The elucidation of structure–permeability relationships for peptide and peptide-like compounds remains a critical need, and cyclic oligomeric depsipeptides[8] provide a powerful platform for filling this gap. The cyclic depsipeptide *ent*-verticilide is the first potent and selective inhibitor of the intracellular calcium channel RyR2 (Fig. 1).[9–11] Its activity has been recapitulated *in vivo* with animal models of disease,[12] and a lower oligomer exhibits similar inhibition.[13] More recent findings indicate a favorable pharmacokinetic–pharmacodynamic (PK–PD) profile.[14] Our interest in defining the pharmacophore through *in vitro* assays[15] led to a broader study to examine molecular features of *ent*-verticilide that enhance or diminish its permeability. Moreover, the study of 'Beyond Rule of 5' (bRo5) molecules, especially macrocyclic compounds, demands a better understanding of their physicochemical properties.[16] The recent report of Sando and coworkers[17] prompts us to report a concomitant investigation comparing the passive permeability[18] of a cyclic depsipeptide, building on similar reports by others[19–22] interested in the physicochemical characteristics (*e.g.* solubility, permeability) of compounds in this size regime.[23,24] Use of a cyclic oligomeric depsipeptide template for this study provided an opportunity to systematically correlate single, double, triple, and quadruple point-replacements of esters in the parent tetradepsipeptide structure with both *N*-H and *N*-Me amides.[15]

[a]*Department of Chemistry, Vanderbilt Institute of Chemical Biology, Vanderbilt University, Nashville, TN 37235-1822, USA. E-mail: jeffrey.n.johnston@vanderbilt.edu*
[b]*Department of Medicine, Vanderbilt Center for Arrhythmia Research and Therapeutics (VanCART), Vanderbilt University Medical Center, Medical Research Bldg IV, Room 1265, 2215B Garland Ave, Nashville, TN 37232-0575, USA*
[c]*Department of Pharmaceutical Sciences, College of Pharmacy, University of Nebraska Medical Center, Omaha, NE 68198, USA*
[d]*Pharmaceutical Sciences Research Center, College of Pharmacy, Lipscomb University, Nashville, TN 37204, USA*

† Electronic supplementary information (ESI) available: Complete experimental details (PDF); NMR data (PDF). See DOI: https://doi.org/10.1039/d4sc02758b

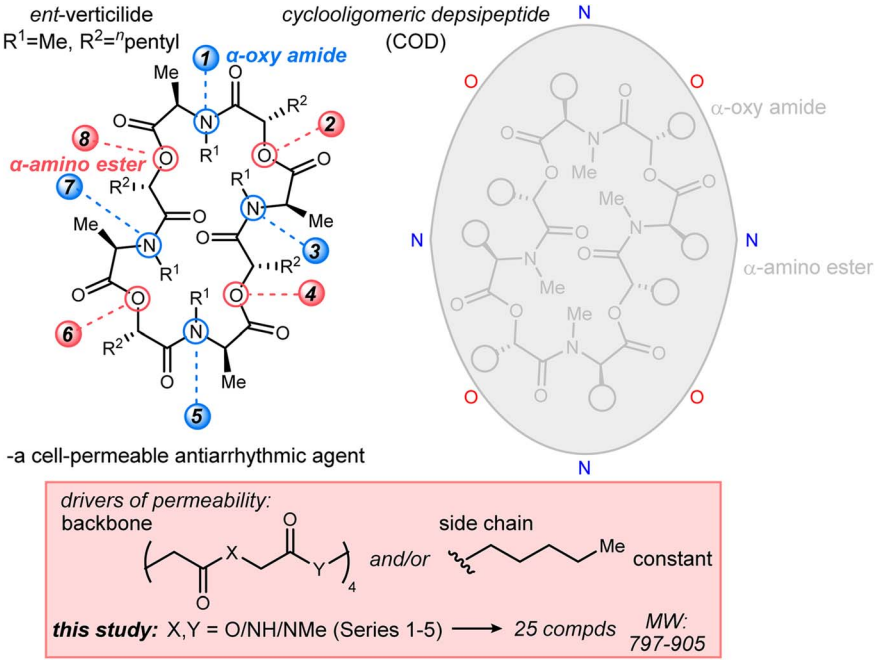

Fig. 1 The *ent*-verticilide cyclooligomeric depsipeptide structure, its general features, and this study's approach to deconvolute the effect of backbone modifications on membrane permeability.

ent-Verticilide and a complete set of 24 analogs over five series (Series 1–5) promised the opportunity to disentangle direct effects of these modifications with potential property-driving changes in conformation, polarity, and hydrogen bonding. An analysis of marketed drugs scrutinized the structural features of oral and injectable drugs, noting that structural differences were more often within the molecular backbones than the side chains of those scaffolds.[25] The combination of ester and amide functional groups in the *ent*-verticilide backbone provides a unique opportunity to further probe the hypothesis that backbone modifications can substantially affect passive permeability independent of side chain modification. Furthermore, the oligomeric nature of *ent*-verticilide provides an additional angle to query to what extent these effects might be additive. We report herein the first outline of common bioisostere interconversions, and correlation of these structural changes with passive permeability. The macrocyclic nature of these depsipeptides and peptides, and their relationship to a cell-permeable antiarrhythmic, broadens the relevance of these findings, increasing the possibility that similar correlations will be identified for use in bRo5 drug development.[26]

Experiment design

The *ent*-verticilide structure is a cyclic tetrameric didepsipeptide, one that offers lipophilic side chains (methyl, pentyl) radiating from a polar core comprised of alternating ester and *N*-Me amides. The molecule is devoid of hydrogen bond donors, and the complexity of its NMR spectrum suggests a high degree of conformational mobility. We posited that this structure provides a platform for determining whether the lipophilic side chains or the moderately polar core drive passive permeability for this compound class. To the best of our knowledge, no study of this size has examined the permeability of compounds systematically to measure the degree to which a polar backbone is a major or minor driver of permeability. To test this hypothesis, five series of backbone modifications were outlined (Fig. 2), each probing the effect of modifying the native esters or *N*-Me amides of the parent *ent*-verticilide, using the industry-standard parallel artificial membrane permeability assay (PAMPA) as a first-pass method to quantify passive permeability.[18] The assay's rudimentary design enabled a high number of replicates and overlapping measurements to arrive at a complete data set with statistical significance. These compounds spanned a molecular weight range of 797–905 g mol^{-1}, with an average of 860 g mol^{-1}.[24,27] Cyclosporin A was used as a cell-permeable positive control.[28]

Series 1: altering *N*-methyl to *N*-H amides while retaining esters

ent-Verticilide lacks hydrogen bond donors, so the first series systematically incorporates *N*-H amides to determine how this modification alters permeability. Series 1 retains the ester lipophilicity while increasing hydrogen bond donors by conversion of *N*-Me to *N*-H amides *via* the alanine residue. Permeable peptides can contain both *N*-Me and *N*-H amides.[29] It is expected that these substitutions will affect the macrocycle conformation, both in major contributor and rate of interconversion among low-lying conformations. It was hypothesized that a higher degree of *N*-methylation will correlate with greater permeability. Literature precedence suggests that *N*-methylation alters permeability by reducing the desolvation penalty for

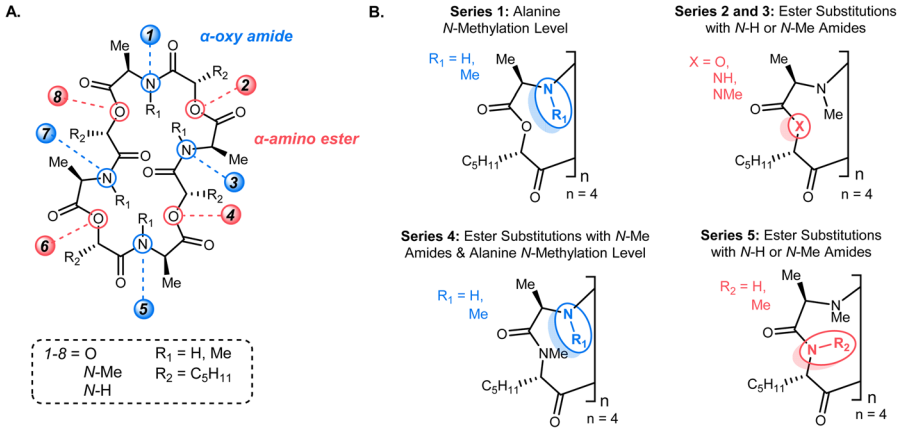

Series	MW (g/mol)	Position[a]	1	2	3	4	5	6	7	8
Series 1: Altering *N*-methyl to *N*-H amides while retaining esters										
ent-vert	853.11		NMe	O	NMe	O	NMe	O	NMe	O
1.1	839.08		NMe	O	NH	O	NMe	O	NMe	O
1.2	825.05	adj	NMe	O	NH	O	NH	O	NMe	O
1.3	825.05	alt	NMe	O	NH	O	NMe	O	NH	O
1.4	811.03		NMe	O	NH	O	NH	O	NH	O
1.5	797.00		NH	O	NH	O	NH	O	NH	O
Series 2: Substitution of esters with *N*-H amides										
2.1	851.56		NMe	O	NMe	NH	NMe	O	NMe	O
2.2	851.14	adj	NMe	O	NMe	NH	NMe	NH	NMe	O
2.3	851.14	alt	NMe	O	NMe	NH	NMe	O	NMe	NH
2.4	850.16		NMe	NH	NMe	NH	NMe	O	NMe	NH
2.5	849.17		NMe	NH	NMe	NH	NMe	NH	NMe	NH
Series 3: Substitution of esters with *N*-Me amides										
3.1	866.15		NMe	O	NMe	NMe	NMe	O	NMe	O
3.2	879.19	adj	NMe	O	NMe	NMe	NMe	NMe	NMe	O
3.3	879.19	alt	NMe	O	NMe	NMe	NMe	O	NMe	NMe
3.4	892.24		NMe	NMe	NMe	NMe	NMe	O	NMe	NMe
3.5	905.28	=4.1, 5.1	NMe	NMe	NMe	NMe	NMe	NMe	NMe	NMe
Series 4: Substitution of esters with *N*-Me amides, and alanine *N*-Me to *N*-H										
4.1	905.28	=3.5, 5.1	NMe	NMe	NMe	NMe	NMe	NMe	NMe	NMe
4.2	891.25		NH	NMe	NMe	NMe	NMe	NMe	NMe	NMe
4.3	877.23	adj	NH	NMe	NH	NMe	NMe	NMe	NMe	NMe
4.4	877.23	alt	NH	NMe	NMe	NMe	NH	NMe	NMe	NMe
4.5	863.20		NH	NMe	NH	NMe	NH	NMe	NMe	NMe
4.6	849.17		NH	NMe	NH	NMe	NH	NMe	NH	NMe
Series 5: Substitution of esters with *N*-H amides										
5.1	905.28	=3.5, 4.1	NMe	NMe	NMe	NMe	NMe	NMe	NMe	NMe
5.2	891.25		NMe	NH	NMe	NMe	NMe	NMe	NMe	NMe
5.3	877.23	adj	NMe	NH	NMe	NMe	NMe	NMe	NMe	NH
5.4	877.23	alt	NMe	NMe	NMe	NH	NMe	NMe	NMe	NH
5.5	863.20		NMe	NH	NMe	NH	NMe	NMe	NMe	NH
5.6	849.17	=2.5	NMe	NH	NMe	NH	NMe	NH	NMe	NH

Fig. 2 (A) The cyclic oligomeric depsipeptide structure highlighting the α-oxy amide and α-amino ester subunits. (B) The backbone atoms therein that are modified systematically to produce Series 1–5 for evaluation of passive permeability by PAMPA assay. [a]For positional isomers with unique depsipeptide or dipeptide residues, adj = modified residues are adjacent, alt = modified residues are alternating. MW: molecular weight (g mol^{-1}).

membrane permeation.[30] Additionally, *N*-H cyclic peptides can form hydrogen bonding networks, and the resulting conformation could affect side chain orientation. Indeed, the solid-state structure for **1.5** revealed intramolecular hydrogen bond acceptor/donor pairs for each consecutive *N*-H amide.[15]

Series 2: substitution of esters with *N*-H amides

This series features a substitution of esters with *N*-H amides while maintaining the naturally occurring *N*-Me amides in the backbone. These modifications increase the polarity and hydrogen bonding which is expected to decrease permeability. By substituting the more lipophilic ester bond with a polar *N*-H amide, the influence of individual esters on overall permeability could be measured concomitant with an increase in hydrogen bonding. Sando and coworkers have shown that some depsipeptides exhibit higher membrane permeability and membrane-retention than their peptide counterparts, which reflects the lipophilicity of the ester relative to *N*-H amide.[17] This is not always the effect, since the mindful design of intramolecular *N*-H amide hydrogen bonding has been advanced as a permeability-enhancing tactic.[21]

Series 3: substitution of esters with *N*-Me amides

This series, like Series 2, increases polarity by replacing esters with amides, but without the addition of hydrogen bond donors. Ester substitution with *N*-Me amides probes the permeability differences between two similar isosteres. With similar bond lengths, bond angles and planar conformations, the differences arise *via* lipophilicity and conformational mobility. Esters are more lipophilic than amides in nature, which suggests that they will have a greater membrane permeability.[31] However, it has been shown that there are some depsipeptides that can be retained by the membrane, which could result in lower permeability.[32]

Series 4: substitution of esters with *N*-Me amides, and alanine *N*-Me to *N*-H

The first all-amide series probes the importance of the alanine *N*-Me amides. Converting all four of the ester bonds to *N*-Me amides creates an all-amide backbone. Presuming that the conversion of all esters to *N*-Me amides will provide similar polarity, but increase conformational flexibility, the demethylation of alanine nitrogen will increase polarity and hydrogen bond donor/acceptor level. It is hypothesized that the increase in *N*-H amides will correspond with decreasing permeability, except when an intramolecular hydrogen bond can form. However, a higher degree of amide methylation could enhance permeability.[33]

Series 5: substitution of esters with *N*-H amides

The second all-amide series focuses again on the ester positions, examining the impact of converting to *N*-H and *N*-Me amides. In this final series, the ester bonds are converted to either *N*-H or *N*-Me amides, while maintaining the naturally occurring *N*-Me amides in the backbone. It is hypothesized that the macrocycles containing more *N*-Me amides will be more permeable than the molecules containing *N*-H amides unless the *N*-H amide is capable of interchange between intra- and intermolecular hydrogen bonding. The addition of hydrogen bond donors subsequently increases polarity, which provides the opportunity for intramolecular hydrogen bonding. This prediction does not account for intramolecular *N*-H amide hydrogen bonding that could bury the polar *N*-H and stabilize a conformation that increases the presentation of nonpolar side chains, or even a two-state system that interconverts between exposed and non-exposed *N*-H amides. It is generally hypothesized that esters exhibit a higher permeability than *N*-H amides, which suggests this series will exhibit lower diffusion than previous series.

Results

The *ent*-verticilide structure exhibits an equal number of esters and *N*-Me amides which are polar hydrogen bond acceptors, but more hydrophobic than *N*-H amides. We hypothesized that the serial replacement of *N*-Me amides with *N*-H amides would decrease passive permeability as measured by P_{app} and % diffusion.[34] This series of five analogs was prepared and analyzed in the PAMPA experiment (Table 1). The analog with two *N*-Me amides and two *N*-H amides can be arranged with the *N*-H amide didepsipeptide monomers adjacent (**1.2**) or in an alternating pattern (**1.3**). As shown in Table 1, each replacement of *N*-Me amide with *N*-H amide(s) resulted in the expected decrease in diffusion. One exception is the analog with all *N*-H amides, as it exhibited an increase in permeability (12% diffusion) relative to its $[NH]_3$ (6% diffusion) and one $[NH]_2$ (5% diffusion) counterparts. The substantial drop in diffusion (19 → 5%) when comparing the alternating $[NH]_2$ analog to its adjacent isomer is also notable. The values for % recovery across this series indicated a consistent level of analyte identification. This series increases the number of HBDs within the COD from 0 (*ent*-verticilide) to 4 (**1.5**).

Series 2 explores the hypothesis that the native ester functionality is beneficial to permeability, but replacement of one or more esters with an *N*-H amide could provide a HBD that might improve permeability by balancing the number of HBAs. A scenario where a fraction of the macrocycle's HBAs are internally bonded by HBDs is envisioned to provide an alternative to intermolecular water solvation. Five analogs were prepared that sequentially replaced each ester with an *N*-H amide, including the double replacement $[NH]_2$ that offers adjacent (**2.2**) and alternating (**2.3**) sequences for the didepsipeptides. A single replacement (**2.1**) increased diffusion substantially from *ent*-verticilide (26 → 37%). This increase held with the adjacent, double replacement as well (**2.2**), increasing diffusion to 30%. The alternating double replacement (**2.3**) exhibited 25% diffusion, and subsequent replacement of esters with *N*-H amides lowered diffusion further (**2.4**: 19%, **2.5**: 18%).

Series 3 is analogous to Series 2, but questions whether replacement of ester with *N*-Me amide (instead of *N*-H amide as in Series 2) will retain or diminish the permeability. The *N*-Me amide provides increased polarity but HBA capability similar to

Table 1 Experimentally-determined permeability measurements using the PAMPA assay for cyclosporin A, *ent*-verticilide, and Series 1–5 compounds[a,b]

	N-Me	*N*-H	log *P*	P_{app} (10^{-6})	log P_{app}	Diffusion (%)	Recovery (%)	HBD	HBA (Est/Am)
CsA[c]	7	4	−8.96	*8.28*	*−5.01*	*28*	86	5	0/11
ent-verticilide	4	0	−8.99	*6.92 ± 0.66*	*−5.21 ± 0.09*	*25.6 ± 2.8*	94	0	4/4
1.1	3	1	−9.18	5.41 ± 0.56	−5.27 ± 0.04	19.4 ± 1.6	91	1	4/4
1.2 (adj)	2	2	−9.14	4.87 ± 0.35	−5.31 ± 0.03	19.0 ± 2.0	88	2	4/4
1.3 (alt)	2	2	−9.82	1.15 ± 0.06	−5.94 ± 0.02	5.1 ± 0.4	91	2	4/4
1.4	1	3	−9.72	1.14 ± 0.23	−5.95 ± 0.09	5.7 ± 1.3	91	3	4/4
1.5	0	4	−9.36	3.51 ± 0.54	−5.46 ± 0.07	12.1 ± 2.5	87	4	4/4
2.1	4	1	−8.82	***12.49 ± 2.49***	***−4.91 ± 0.09***	***36.9 ± 4.6***	88	1	3/5
2.2 (adj)	4	2	−8.94	***9.04 ± 0.71***	***−5.05 ± 0.03***	***30.4 ± 2.3***	89	2	2/6
2.3 (alt)	4	2	−9.03	*5.93 ± 0.51*	*−5.23 ± 0.04*	*25.0 ± 1.6*	90	2	2/6
2.4	4	3	−9.17	4.76 ± 0.75	−5.33 ± 0.07	19.1 ± 2.3	89	3	1/7
2.5	4	4	−9.14	4.87 ± 0.48	−5.31 ± 0.04	17.5 ± 2.3	86	4	0/8
3.1	5	0	−9.09	*6.14 ± 0.80*	*−5.22 ± 0.05*	*22.4 ± 2.6*	84	0	3/5
3.2 (adj)	6	0	−9.18	4.28 ± 0.40	−5.37 ± 0.04	18.6 ± 2.4	94	0	2/6
3.3 (alt)	6	0	−9.21	3.32 ± 0.24	−5.48 ± 0.03	17.2 ± 0.9	91	0	2/6
3.4	7	0	−9.32	3.81 ± 0.32	−5.42 ± 0.04	12.9 ± 0.9	93	0	1/7
3.5	8	0	−9.43	2.83 ± 0.40	−5.55 ± 0.06	11.0 ± 2.2	90	0	0/8
4.1 (=3.5, 5.1)	8	0	−9.43	2.83 ± 0.40	−5.55 ± 0.06	11.0 ± 2.2	90	0	0/8
4.2	7	1	−9.15	4.78 ± 0.41	−5.32 ± 0.04	19.9 ± 1.7	89	1	0/8
4.3 (adj)	6	2	−9.20	4.05 ± 0.24	−5.39 ± 0.03	18.0 ± 1.5	91	2	0/8
4.4 (alt)	6	2	−9.42	2.13 ± 0.18	−5.68 ± 0.04	11.3 ± 0.7	92	2	0/8
4.5	5	3	−9.52	1.50 ± 0.15	−5.83 ± 0.04	9.0 ± 1.0	88	3	0/8
4.6	4	4	−9.93	0.34 ± 0.07	−6.48 ± 0.08	<5	91	4	0/8
5.1 (=3.5, 4.1)	8	0	−9.43	2.83 ± 0.40	−5.55 ± 0.06	11.0 ± 2.2	90	0	0/8
5.2	7	1	−9.10	*5.73 ± 0.38*	*−5.24 ± 0.03*	*23.8 ± 1.5*	91	1	0/8
5.3 (adj)	6	2	−9.14	*3.81 ± 0.32*	*−5.42 ± 0.04*	*20.9 ± 2.1*	90	2	0/8
5.4 (alt)	6	2	−9.26	4.01 ± 0.45	−5.40 ± 0.05	15.9 ± 2.4	90	2	0/8
5.5	5	3	−9.42	2.73 ± 0.35	−5.57 ± 0.06	10.0 ± 2.1	88	3	0/8
5.6 (=2.5)	4	4	−9.14	4.87 ± 0.48	−5.31 ± 0.04	17.5 ± 2.3	86	4	0/8

[a] Definitions: *N*-Me: *N*-Me amide count in structure; *N*-H: *N*-H amide count in structure; log *P*: determined from standard curve to measure [D] and [A], using equation detailed in SI 2.4b; P_{app}: determined from a ratio-based method, given as mean ± standard deviation; diffusion: [acceptor]/[acceptor + donor]; recovery: acceptor + donor/total analyte; HBD: potential hydrogen bond donor; HBA: potential hydrogen bond acceptor, Est: ester, Am: amide. Italic font highlights compounds of higher permeability: bold italic ≥ 30% diffusion, non-bold italic = 20–30% diffusion. [b] General details describing methods and analysis, including standard deviation, are in the ESI. [c] For reference, cyclosporin A is a cell-permeable immunosuppressant with 4 *N*-H and 7 *N*-Me amides. The *N*-H amides combine with one hydroxyl for a total of 5 HBDs. Also for CsA, 11 amides and one hydroxyl provide a total of 12 HBAs.

an ester. The increased conformational mobility of tertiary amide, relative to ester, might lead to nuanced effects on the compound's ability to diffuse through the membrane. Based on these expectations, the diffusion profile for this series was perhaps narrower than expected (22 → 11%) but followed a nearly linear decrease in diffusion with each replacement of ester for *N*-Me amide. This includes a 3% decrease from $[NH]_1$ (**3.1**) to adjacent-$[NH]_2$ (**3.2**), and a further 2% decrease for alternating-$[NH]_2$ (**3.3**). Since the replacement of an ester for *N*-Me amide does not alter the HBA or HBD qualities, it is tempting to use this trend to propose a 2–4% decrease in diffusion for ester → *N*-Me amide replacement. Conversely, the *N*-Me → ester replacement may provide a 2–4% increase in diffusion, similar to the recent findings of Sando.[17]

Peptide Series 4 design includes the replacement of esters (of parent *ent*-verticilide) with *N*-Me amides, while investigating the demethylation of alanine nitrogen to probe the effect of an increase in polarity and HBD/HBA level. Compared to the parent all-*N*-Me peptide **4.1** (11% diffusion), analog **4.2** provided a positive spike in permeability, at 20% diffusion. A second replacement of *N*-Me for *N*-H sustained this spike (**4.3**, 18% diffusion), suggesting that internal hydrogen bonding may both attenuate the increase in hydrophilicity and encourage a more lipophilic conformation. Further *N*-Me to *N*-H conversion provided regular decreases in diffusion (**4.4–4.6**), with a 3 *N*-H : 5 *N*-Me ratio providing 9% diffusion, and a 4 : 4 ratio delivering diffusion below the limit of detection.

Series 5 explores substitution of the esters with combinations of *N*-Me and *N*-H amides, beginning from the all-*N*-Me analog **3.5** (relabeled **5.1**). Analog **3.5**/**4.1**/**5.1** was among those with the poorest passive diffusion (see also **1.3**, **1.4**). A single *N*-H amide among seven *N*-Me amides provided analog **5.2** with diffusion restored to 24%, nearly equivalent to *ent*-verticilide. Two *N*-H amides among 6 *N*-Me amides was slightly less membrane-permeable in the adjacent isomer (**5.3**). The alternating positional isomer (**5.4**) exhibited diminished permeability (16%). The lowest permeability in this Series was observed with **5.5** (11% diffusion) at a 5 : 3 *N*-Me/*N*-H ratio, whereas replacing a fourth *N*-Me amide with *N*-H resulted in an analog with 18% diffusion. Interestingly, this *N*-Me/*N*-H amide

analog **5.6** is the same as **2.5**, which was the least permeable analog in Series 2, although its Series 2 analogs collectively exhibited good permeability.

Observations and discussion

This relatively comprehensive data set generated from systematic changes to the backbone of *ent*-verticilide was used to identify structure–permeability correlations. The passive permeability ranged from <5% (**1.4**, **4.6**) to 37% (**2.1**) diffusion across a total of 24 analogs of *ent*-verticilide prepared and measured in Series 1–5 (Fig. 3). This range extends in both more- and less-permeable directions relative to *ent*-verticilide (26%) and cyclosporin A (28%).

• The number of hydrogen bond donors (HBDs) in a macrocycle does not always negatively affect permeability. Compounds with the maximal number (4 HBDs) of *N*-H amides ranged from 12% (**1.5**) to 18% diffusion (**2.5**, **5.6**), compared to the least permeable compounds **1.3** (2 HBDs) and **1.4** (3 HBDs).

• Within a series containing no HBDs, but varying relative ester/amide content, permeability generally increased as ester content increased from 11% for all-*N*-Me amide (**3.5**) to 22% for 3 esters/5 *N*-Me amides (**3.1**). This trend mirrors that identified in Sando's recent study.[17]

• The ester content alone does not drive permeability. Compound *ent*-verticilide (4 esters, 26%) was at the high-permeability range, while **1.4** (4 esters, 6%) exhibited the lowest permeability of 24 analogs.

• Considering the compounds composed only of HBAs, higher permeability correlated with a balance between ester and *N*-Me amide (*ent*-vert, 26%; **3.1**, 22%), whereas those with a ratio favoring *N*-Me amides over esters exhibited lower permeability (2 ester:6 *N*-Me amide: **3.2**, 19%; **3.3**, 17%; 1 ester:7 *N*-Me amide: **3.4**, 13%; only *N*-Me amide: **3.5**, 11%).

• Considering the compounds that offered a symmetry element, resulting in the possibility of adjacent or alternating positioning of the unique didepsipeptides (4 pairs: **1.2**/**1.3**, **2.2**/**2.3**, **3.2**/**3.3**, **5.3**/**5.4**), all adjacent isomers exhibited higher permeability (>19%), while all alternating isomers exhibited lower permeability (<16%) with one exception (**2.3**, 23%).

• All high *N*-H-content compounds (4 HBDs) were in the lower half of permeability measured (<18%). However, the absence of *N*-H-content did not at all correlate with a permeability trend: *ent*-vert, **3.1**, and **3.2** were >18% diffusion, while **3.3**, **3.4**, and **3.5** were <17% diffusion.

ent-Verticilide's eight residues are simplified by its oligomeric nature [α-hydroxy-heptamide-D-Ala], providing key differences in size and symmetry, both of which offer additional analogs and data for passive membrane permeability. The Sando study focused on a cyclic hexapeptide (Tyr-Leu-^{D}Leu-Leu-Leu-^{D}Pro) model selected for its known low membrane permeability, finding that replacement of *N*-H amide at any position except ^{D}Leu3 enhanced permeability. Double substitutions or higher were not explored. Paradoxically, these permeability-increasing substitutions involved both solvent-exposed and unexposed *N*-H amides. Sando also showed that the amide-to-ester substitution has little conformational effect, while an *N*-Me amide substitution changed the conformation significantly but, in this case, did not change the number of solvent-exposed *N*-H amides.

The symmetry of *ent*-verticilide provides possible compensatory interactions *via* distal functional groups. One finding is consistent: the ester functional group can provide enhanced membrane permeability despite the presence of other *N*-H or *N*-

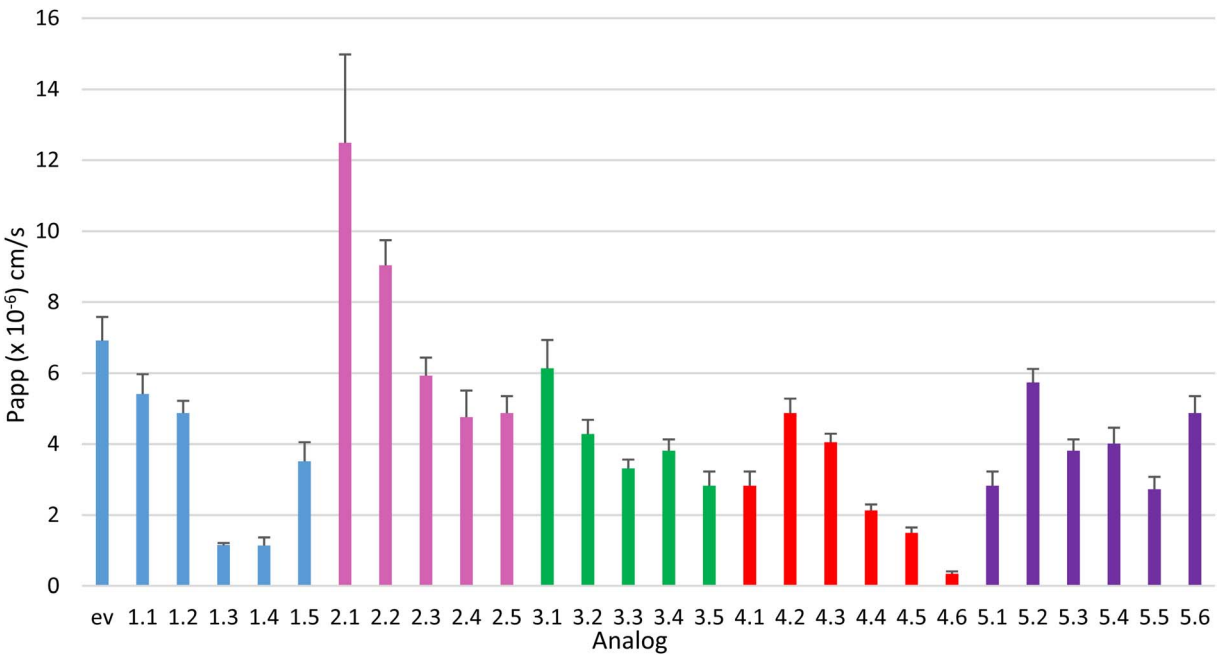

Fig. 3 Experimental P_{app} values for Series 1 (blue), 2 (pink), 3 (green), 4 (red) and 5 (purple). $^{a}P_{app}$: determined from a ratio-based method, provided as a mean with the error bars being standard deviation.

Me amides. However, the template studied here addresses the potential synergism between residues across the macrocycle, including the possible compensatory role a residue may play to drive permeability retention. Compensatory behavior may result in the chameleon characteristic often invoked for some peptides (*i.e.* cyclosporin A)[35] where a conformational change is believed to interconvert exposed and unexposed functionality as needed for transition from aqueous to membrane to aqueous environments to enter a cell.[21,36] This may contribute to the finding here that introduction of a single *N*-H amide, at the expense of an ester, led to the analog with highest passive permeability (**2.1**). The second-highest permeability was found in an analog where two *N*-H amides (adjacent didepsipeptides) replaced two esters (**2.2**), and its non-adjacent isomer was essentially equipermeable to *ent*-verticilide. Importantly, the solid-state structure for *N*-H *ent*-verticilide (**1.5**) reveals a conformation that presents an all-pentyl lipophilic face on one side of the ring plane, and an all-methyl face on the opposite side.[13] Within the 24-membered ring backbone of **1.5**, two of the four *N*-H amides form intramolecular hydrogen bonds with ester carbonyls, while the remaining two are solvent-exposed (Fig. 4).

In these cases, the beneficial effect of amide *N*-methylation can be scaffold-dependent. In others, the effect of methylation may be more nuanced. For example, analog **1.5** exhibits two intramolecular *N*-H···O=C intramolecular H-bonds, and two solvent-exposed amide *N*-H bonds.[13] While it is true that *N*-methylation of each amide increases permeability, the change is rather abrupt from low permeability (**1.3**/**1.4**/**1.5**) to moderate permeability (*ent*-verticilide/**1.1**/**1.2**). Analog **1.3** is especially peculiar, since it has two intramolecular H-bonds that can form analogous to **1.5**, leaving two solvent-exposed *N*-Me amides. This network should lead to good permeability, but it does not (5% diffusion). Similarly, analog **1.2** can engage in an intramolecular hydrogen bond with one *N*-H amide, while the other would be solvent-exposed. Permeability of this analog was similar to **1.1** whose 'exposed' amide is an *N*-Me (19% *vs.* 20% diffusion).

Some inter-Series observations are important. In all Series, substantially better diffusion was exhibited by the adjacent positional isomers. For example, a comparison of adjacent

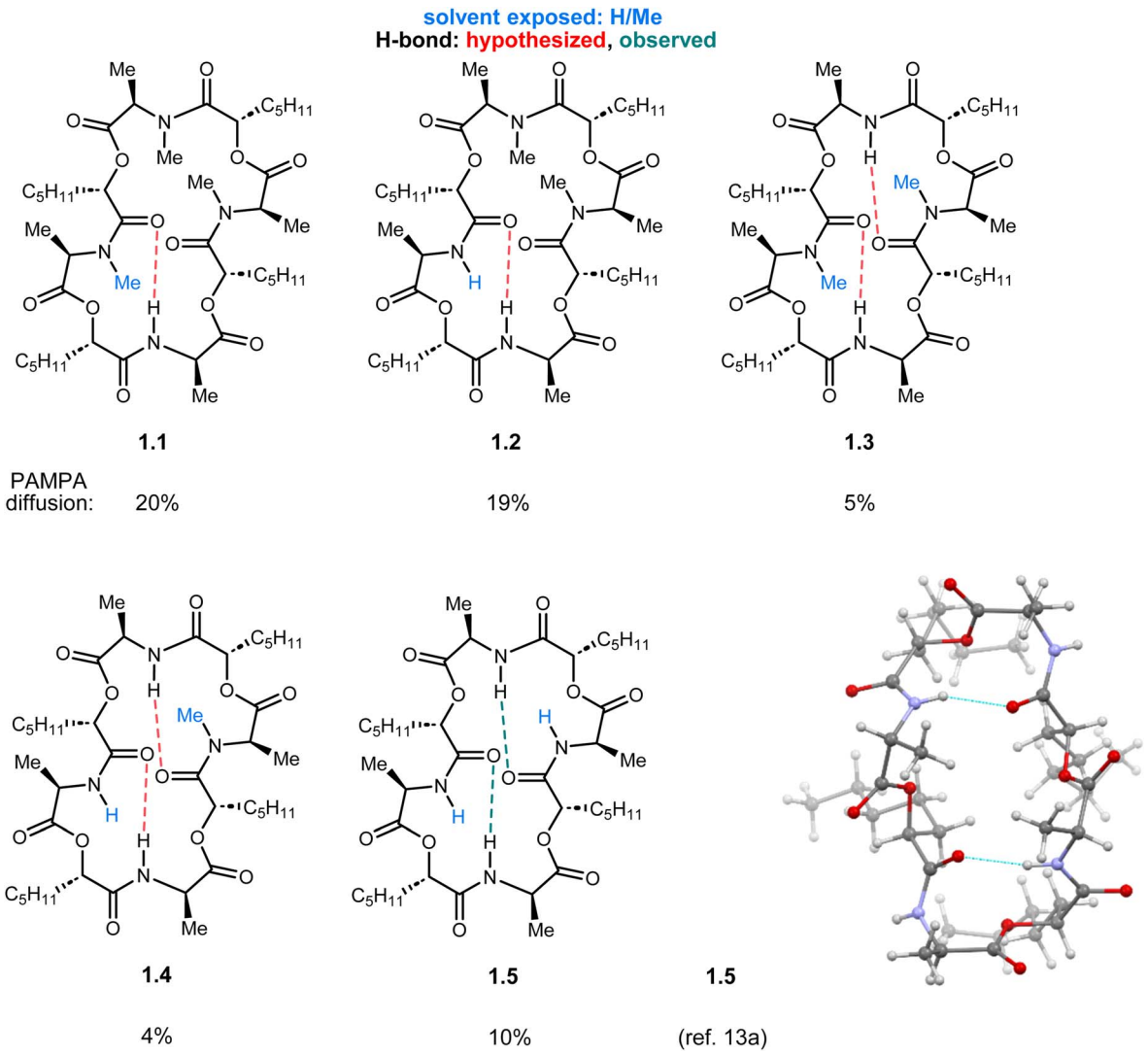

Fig. 4 Comparison of Series 1 analogs with a map of hypothesized hydrogen bonds based on the solid-state structure of **1.5**.

analog **1.2** to the alternating isomer (**1.3**) in Series 1 revealed a 19% *vs.* 5% diffusion. This is a rather dramatic example where the "total polar content" of the backbone alone does not drive permeability. Instead, its arrangement within the structure can either preserve or diminish its diffusion properties. This trend was observed in all other cases as well, with 30% *vs.* 25%, 19% *vs.* 17%, 18% *vs.* 11%, and 21% *vs.* 16% for Series 2–5, respectively.

Series 3 suggests that ester and *N*-Me amide functionality may be somewhat interchangeable with an increase in diffusion associated with the ester. This behavior mirrors that reported recently.[17] However, this correlation may only hold when the overall HBA/HBD content is unchanged, as it was in Series 3.

Series 2 provided both the highest level of increased permeability for an analog (**2.1**), and the broadest range of passive diffusion (18–37%) *via* decreasing ester content by converting the depsipeptide to a mixed *N*-Me/*N*-H peptide. Unlike the trend noted in Series 3, this trend is opposite to recent findings that increasing ester content beginning from a peptide always improves passive permeability. Such an effect may be more nuanced, with some combination of backbone ester/*N*-Me/*N*-H amide constitution driving optimal permeability. The remaining Series provided somewhat similar overall ranges of diffusion: 10, 13, ~13, and 14 for Series 1, 3–5 respectively. Such a consistent range might lead one to speculate that the backbone composition has an ultimately limited effect, but the unmeasurable permeability for **4.6** clearly demonstrates the dominance of backbone over aliphatic side chains.

Caco-2 assays

Select compounds ranging in passive PAMPA permeabilities were evaluated using the Caco-2 assay (Fig. 5). Atenolol (10 μM) and metoprolol (10 μM) were included in the assay as a low and high passive permeability reference compound with a P_{app} (A–B) of 0.121 and 19.8, respectively. Digoxin, a model P-gp substrate used to assess transport-mediated permeability, exhibited a P_{app} (A–B) of 1.59 and a P_{app} (B–A) of 12.2 with an efflux ratio of 7.68. *ent*-Verticilide exhibited low permeability with a P_{app} (A–B) of 0.604 and a P_{app} (B–A) of 0.964. With an efflux ratio of 1.60, there was no evidence efflux-mediated transport of *ent*-verticilide.

Depsipeptide **1.5** is the all-*N*–H analog of *ent*-verticilide that exhibited attenuated diffusion (12%) as expected relative to *ent*-verticilide (26%). Its evaluation in the Caco-2 assay revealed a P_{app} (A–B) = 0.186, consistent with attenuated diffusion, and a 0.482 efflux ratio. Series 2 was chosen for complete evaluation since this series displayed a near-linear trend and expanded passive permeability in PAMPA (37% → 18% diffusion) for analogs **2.1** → **2.5**. These analogs sequentially replaced the esters in verticilide with *N*-H amides, with the expected decrease in PAMPA permeability. In the Caco-2 assay, P_{app} (A–B) values were 0.978, 0.349, ND,[37] 2.28, 2.89 for **2.1–2.5**, respectively (Fig. 5).

Evidence for transport-mediated efflux was observed for **2.2** with an efflux ratio of 6.09. Analog **3.5** was also evaluated in Caco-2 as a low-permeability peptide analog with all *N*-Me amides since methylation of amides is known to improve permeability. Analog **3.5** exhibited moderate permeability in Caco-2 with P_{app} (A–B) = 1.99 and an efflux ratio of 0.928. Overall, both the Caco-2 and PAMPA data generally indicate that these select analogs were generally low to moderate permeability compounds. However, P_{app} estimates in the PAMPA assay were consistently higher for each compound than observed in the Caco-2 assay. From an absolute permeability perspective two distinct groupings were noted. Group 1 (*ent*-verticilide, **1.5**, **2.1**) whose permeability values by PAMPA were higher relative to Group 2 (**2.4**, **2.5**, **3.5**). This permeability relationship was inverted in the Caco-2 assay with compounds in Group 2 exhibiting higher permeability values compared to compounds in Group 1. However, a similar rank order of permeability was observed within Group 1 (**2.1** > *ent*-verticilide > **1.5**) and Group 2 (**2.5** > **2.4** > **3.5**) for both the PAMPA and Caco-2 assay. Compound **2.2** or **2.3** could not be evaluated in the absolute or relative permeability comparisons due to a high efflux ratio and undetectable compound levels, respectively, in the Caco-2 assay. Overall, differences in permeability between the two assays most likely reflect the differences inherent among them, specifically passive *vs.* transport-mediated behavior.

compound	P_{app} (x 10^{-6} cm/sec)		ER
	A-B	B-A	
atenolol	0.121	0.482	3.98
metoprolol	19.8	15.4	0.78
digoxin	1.59	12.2	7.68
ent-verticilide	0.604	0.964	1.60
1.5	0.186	0.0896	0.48
2.1	0.978	1.16	1.18
2.2	0.349	2.12	6.09
2.3	ND	ND	ND
2.4	2.28	4.32	1.89
2.5	2.89	6.82	2.36
3.5	1.99	1.85	0.93

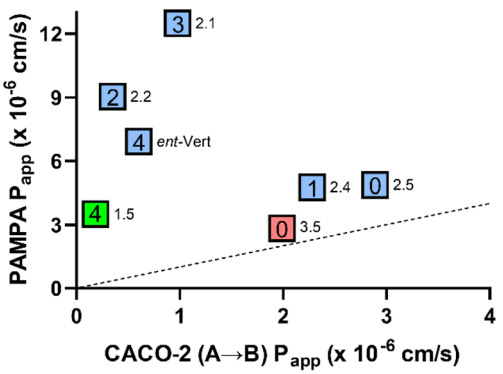

Fig. 5 Assay of select compounds by Caco-2 permeability assay (left) and PAMPA/Caco-2 permeability correlation plot (right). [a]General details describing methods and analysis are in the ESI.† Donor concentration (Caco-2) = 10 μM. ND = not detectable. ER = efflux ratio (AB/BA). Right panel: the number of ester functional groups for each compound is listed inside the box. Colors highlight compounds in different Series (green = Series 1, blue = Series 2, red = Series 3). Only compounds with both PAMPA and Caco-2 measurements are included. Dotted line indicates [PAMPA/Caco-2] = 1. PAMPA data is summarized in Table 1.

Conclusion

An understanding of the extent to which the polar backbone of polymeric therapeutics (*i.e.* peptides) can drive passive membrane permeability is critical to the rational development of new bRo5 therapeutics with desirable physicochemical properties. Within peptidic structures, the relative contribution of ester, *N*-methyl amide, and *N*-H amide functionality to passive permeability is emerging as a possible variable to manipulate pharmacologic permeability.[17,19] Cyclic peptides offer conformationally-limited templates in which to study the ratio of backbone : side chain polarity.[38,39]

Using the octadepsipeptide *ent*-verticilide lead, we prepared 24 analogs, within a relatively narrow molecular weight range, and measured the passive permeability of each using PAMPA. Numerous trends emerged that highlight the ability to substantively modify – either enhance or decrease – passive permeability without side chain modification. In one case, P_{app} increased 80% over *ent*-verticilide by the non-intuitive replacement of one backbone ester for an *N*-H amide. The overall trends can be used as a critical informer study to prioritize specific backbone modifications in peptide drug development. For example, for cases when ester-to-amide substitution reduces inhibitory activity in cells but not *in vitro*, the ability to disentangle passive permeability effects could speed further development. Overall, this study provides a rigorous starting point for understanding the relative contributions of polar backbones with lipophilic side chains in a manner that could be leveraged in optimization studies with non-oligomeric lead compounds. The molecular basis for these behaviors is the subject of ongoing studies and will be reported in due course.

Materials and methods

Synthesis

Series 1–5 were prepared by chemical synthesis and purified using silica gel chromatography to arrive at material that was >95% pure by ^{1}H NMR spectroscopy and/or HPLC analysis, described elsewhere.[40]

PAMPA

The permeability assay across an artificial membrane was completed using literature procedures[18b] and details are provided in ESI.†

Caco-2 transport studies

Polarized human colorectal adenocarcinoma-derived (Caco-2) cells were used and details are provided in ESI.†

Data availability

Full experimental details for all assays and data analysis are provided. All supplementary data for this article can be found in the ESI.†

Author contributions

MPT, ANS, and JNJ designed the research, MPT performed the research, MPT, DJB, CRH, WSA, JNJ analyzed the results, and MPT, WSA, JNJ wrote the paper with input from all authors.

Conflicts of interest

The authors declare no competing financial interest.

Acknowledgements

Research reported in this publication was supported by the National Heart, Blood, and Lung Institute of the National Institutes of Health (NIH R01 HL151223, HL164064 and HL151125 (F31 support for MPT and ANS)) and the PhRMA Foundation Postdoctoral Fellowship (DJB support). We're grateful to Dr Jaru Taechalertpaisarn and Prof. Scott Lokey for helpful early guidance to extend their published protocols to these studies.

References

1 (*a*) M.-J. Blanco, K. M. Gardinier and M. N. Namchuk, Advancing New Chemical Modalities into Clinical Studies, *ACS Med. Chem. Lett.*, 2022, **13**, 1691–1698; (*b*) M.-J. Blanco, in *Cyclic Peptide Design*, ed. G. Goetz, Springer New York, New York, NY, 2019, pp. 203–233.

2 A. Henninot, J. C. Collins and J. M. Nuss, The Current State of Peptide Drug Discovery: Back to the Future?, *J. Med. Chem.*, 2018, **61**, 1382–1414.

3 F. Giordanetto and J. Kihlberg, Macrocyclic Drugs and Clinical Candidates: What Can Medicinal Chemists Learn from Their Properties?, *J. Med. Chem.*, 2014, **57**, 278–295.

4 J. L. Hickey, D. Sindhikara, S. L. Zultanski and D. M. Schultz, Beyond 20 in the 21st Century: Prospects and Challenges of Non-canonical Amino Acids in Peptide Drug Discovery, *ACS Med. Chem. Lett.*, 2023, **14**, 557–565.

5 M. R. Naylor, A. T. Bockus, M.-J. Blanco and R. S. Lokey, Cyclic peptide natural products chart the frontier of oral bioavailability in the pursuit of undruggable targets, *Curr. Opin. Chem. Biol.*, 2017, **38**, 141–147.

6 P. G. Dougherty, A. Sahni and D. Pei, Understanding Cell Penetration of Cyclic Peptides, *Chem. Rev.*, 2019, **119**, 10241–10287.

7 Selected examples: (*a*) H. Salim, J. Song, A. Sahni and D. Pei, Development of a Cell-Permeable Cyclic Peptidyl Inhibitor against the Keap1–Nrf2 Interaction, *J. Org. Chem.*, 2020, **85**, 1416–1424; (*b*) M. Tanada, M. Tamiya, A. Matsuo, A. Chiyoda, K. Takano, T. Ito, M. Irie, T. Kotake, R. Takeyama, H. Kawada, R. Hayashi, S. Ishikawa, K. Nomura, N. Furuichi, Y. Morita, M. Kage, S. Hashimoto, K. Nii, H. Sase, K. Ohara, A. Ohta, S. Kuramoto, Y. Nishimura, H. Iikura and T. Shiraishi, Development of Orally Bioavailable Peptides Targeting an Intracellular Protein: From a Hit to a Clinical KRAS Inhibitor, *J. Am. Chem. Soc.*, 2023, **145**, 16610.

8 P. A. Trinidad-Calderón, C. D. Varela-Chinchilla and S. García-Lara, Depsipeptides Targeting Tumor Cells: Milestones from In Vitro to Clinical Trials, *Molecules*, 2023, **28**, 670.

9 S. M. Batiste, D. J. Blackwell, K. Kim, D. O. Kryshtal, N. Gomez-Hurtado, R. T. Rebbeck, R. L. Cornea, J. N. Johnston and B. C. Knollmann, Unnatural verticilide enantiomer inhibits type 2 ryanodine receptor-mediated calcium leak and is antiarrhythmic, *Proc. Natl. Acad. Sci. U. S. A.*, 2019, **116**, 4810–4815.

10 C. J. M. v. Opbergen, N. Bagwan, S. R. Maurya, J.-C. Kim, A. N. Smith, D. J. Blackwell, J. N. Johnston, B. C. Knollmann, M. Cerrone, A. Lundby and M. Delmar, Exercise Causes Arrhythmogenic Remodeling of Intracellular Calcium Dynamics in Plakophilin-2-Deficient Hearts, *Circulation*, 2022, **145**, 1480–1496.

11 J. Šeflová, J. A. Schwarz, A. N. Smith, B. Svensson, D. J. Blackwell, T. A. Phillips, R. Nikolaienko, E. Bovo, R. T. Rebbeck, A. V. Zima, D. D. Thomas, F. Van Petegem, B. C. Knollmann, J. N. Johnston, S. L. Robia and R. L. Cornea, RyR2 Binding of an Antiarrhythmic Cyclic Depsipeptide Mapped Using Confocal Fluorescence Lifetime Detection of FRET, *ACS Chem. Biol.*, 2023, **18**, 2290–2299.

12 K. Kim, D. J. Blackwell, S. L. Yuen, M. P. Thorpe, J. N. Johnston, R. L. Cornea and B. C. Knollmann, The selective RyR2 inhibitor ent-verticilide suppresses atrial fibrillation susceptibility caused by Pitx2 deficiency, *J. Mol. Cell. Cardiol.*, 2023, **180**, 1–9.

13 (*a*) A. N. Smith, D. J. Blackwell, B. C. Knollmann and J. N. Johnston, Ring Size as an Independent Variable in Cyclooligomeric Depsipeptide Antiarrhythmic Activity, *ACS Med. Chem. Lett.*, 2021, **12**, 1942–1947; (*b*) A. Gochman, T. Q. Do, K. Kim, J. A. Schwarz, M. P. Thorpe, D. J. Blackwell, P. Ritschel, A. N. Smith, R. T. Rebbeck, W. S. Akers, R. L. Cornea, D. R. Laver, J. N. Johnston and B. C. Knollmann, ent-Verticilide B1 inhibits type 2 ryanodine receptor channels and is antiarrhythmic in Casq2-/- mice, *Mol. Pharmacol.*, 2024, **105**, 194–201.

14 D. J. Blackwell, A. N. Smith, T. Do, A. Gochman, J. Schmeckpeper, C. R. Hopkins, W. S. Akers, J. N. Johnston and B. C. Knollmann, In Vivo Pharmacokinetic and Pharmacodynamic Properties of the Antiarrhythmic Molecule ent-Verticilide, *J. Pharmacol. Exp. Ther.*, 2023, **385**, 205.

15 A. N. Smith, M. P. Thorpe, D. J. Blackwell, S. M. Batiste, C. R. Hopkins, N. D. Schley, B. C. Knollmann and J. N. Johnston, Structure–Activity Relationships for the N-Me- Versus N-H-Amide Modification to Macrocyclic ent-Verticilide Antiarrhythmics, *ACS Med. Chem. Lett.*, 2022, **13**, 1755–1762.

16 J. Moxam, S. Naylon, A. D. Richaud, G. Zhao, A. Padilla and S. P. Roche, Passive Membrane Permeability of Sizable Acyclic β-Hairpin Peptides, *ACS Med. Chem. Lett.*, 2023, **14**, 278–284.

17 Y. Hosono, S. Uchida, M. Shinkai, C. E. Townsend, C. N. Kelly, M. R. Naylor, H.-W. Lee, K. Kanamitsu, M. Ishii, R. Ueki, T. Ueda, K. Takeuchi, M. Sugita, Y. Akiyama, S. R. Lokey, J. Morimoto and S. Sando, Amide-to-ester substitution as a stable alternative to N-methylation for increasing membrane permeability in cyclic peptides, *Nat. Commun.*, 2023, **14**, 1416.

18 (*a*) M. Kansy, F. Senner and K. Gubernator, Physicochemical High Throughput Screening: Parallel Artificial Membrane Permeation Assay in the Description of Passive Absorption Processes, *J. Med. Chem.*, 1998, **41**, 1007–1010; (*b*) M. H. Oh, H. J. Lee, S. H. Jo, B. B. Park, S.-B. Park, E.-y. Kim, Y. Zhou, Y. H. Jeon and K. Lee, Development of Cassette PAMPA for Permeability Screening, *Biol. Pharm. Bull.*, 2017, **40**, 419–424.

19 Y. Li, N. P. Lavey, J. A. Coker, J. E. Knobbe, D. C. Truong, H. Yu, Y.-S. Lin, S. L. Nimmo and A. S. Duerfeldt, Consequences of Depsipeptide Substitution on the ClpP Activation Activity of Antibacterial Acyldepsipeptides, *ACS Med. Chem. Lett.*, 2017, **8**, 1171–1176.

20 H. Miyachi, K. Kanamitsu, M. Ishii, E. Watanabe, A. Katsuyama, S. Otsuguro, F. Yakushiji, M. Watanabe, K. Matsui, Y. Sato, S. Shuto, T. Tadokoro, S. Kita, T. Matsumaru, A. Matsuda, T. Hirose, M. Iwatsuki, Y. Shigeta, T. Nagano, H. Kojima, S. Ichikawa, T. Sunazuka and K. Maenaka, Structure, solubility, and permeability relationships in a diverse middle molecule library, *Bioorg. Med. Chem. Lett.*, 2021, **37**, 127847.

21 G. Bhardwaj, J. O'Connor, S. Rettie, Y.-H. Huang, T. A. Ramelot, V. K. Mulligan, G. G. Alpkilic, J. Palmer, A. K. Bera, M. J. Bick, M. Di Piazza, X. Li, P. Hosseinzadeh, T. W. Craven, R. Tejero, A. Lauko, R. Choi, C. Glynn, L. Dong, R. Griffin, W. C. van Voorhis, J. Rodriguez, L. Stewart, G. T. Montelione, D. Craik and D. Baker, Accurate de novo design of membrane-traversing macrocycles, *Cell*, 2022, **185**, 3520–3532.

22 A. Le Roux, É. Blaise, P.-L. Boudreault, C. Comeau, A. Doucet, M. Giarrusso, M.-P. Collin, T. Neubauer, F. Kölling, A. H. Göller, L. Seep, D. T. Tshitenge, M. Wittwer, M. Kullmann, A. Hillisch, J. Mittendorf and E. Marsault, Structure–Permeability Relationship of Semipeptidic Macrocycles—Understanding and Optimizing Passive Permeability and Efflux Ratio, *J. Med. Chem.*, 2020, **63**, 6774–6783.

23 H. Verma, B. Khatri, S. Chakraborti and J. Chatterjee, Increasing the bioactive space of peptide macrocycles by thioamide substitution, *Chem. Sci.*, 2018, **9**, 2443–2451.

24 P. Matsson and J. Kihlberg, How Big Is Too Big for Cell Permeability?, *J. Med. Chem.*, 2017, **60**, 1662–1664.

25 M. Vieth, M. G. Siegel, R. E. Higgs, I. A. Watson, D. H. Robertson, K. A. Savin, G. L. Durst and P. A. Hipskind, Characteristic Physical Properties and Structural Fragments of Marketed Oral Drugs, *J. Med. Chem.*, 2004, **47**, 224–232.

26 B. Over, P. Matsson, C. Tyrchan, P. Artursson, B. C. Doak, M. A. Foley, C. Hilgendorf, S. E. Johnston, M. D. Lee, R. J. Lewis, P. McCarren, G. Muncipinto, U. Norinder, M. W. D. Perry, J. R. Duvall and J. Kihlberg, Structural and

conformational determinants of macrocycle cell permeability, *Nat. Chem. Biol.*, 2016, **12**, 1065–1074.

27 (*a*) C. R. Pye, W. M. Hewitt, J. Schwochert, T. D. Haddad, C. E. Townsend, L. Etienne, Y. Lao, C. Limberakis, A. Furukawa, A. M. Mathiowetz, D. A. Price, S. Liras and R. S. Lokey, Nonclassical Size Dependence of Permeation Defines Bounds for Passive Adsorption of Large Drug Molecules, *J. Med. Chem.*, 2017, **60**, 1665–1672; (*b*) M. Kansy, H. Fischer, K. Kratzat, F. Senner, B. Wagner and I. Parrilla, in *Pharmacokinetic Optimization in Drug Research*, 2001, pp. 447–464.

28 P. F. Augustijns, T. P. Bradshaw, L. S. L. Gan, R. W. Hendren and D. R. Thakker, Evidence for a Polarized Efflux System in Caco-2 Cells Capable of Modulating Cyclosporine A Transport, *Biochem. Biophys. Res. Commun.*, 1993, **197**, 360–365.

29 (*a*) T. Rezai, B. Yu, G. L. Millhauser, M. P. Jacobson and R. S. Lokey, Testing the Conformational Hypothesis of Passive Membrane Permeability Using Synthetic Cyclic Peptide Diastereomers, *J. Am. Chem. Soc.*, 2006, **128**, 2510–2511; (*b*) T. A. Hill, R.-J. Lohman, H. N. Hoang, D. S. Nielsen, C. C. G. Scully, W. M. Kok, L. Liu, A. J. Lucke, M. J. Stoermer, C. I. Schroeder, S. Chaousis, B. Colless, P. V. Bernhardt, D. J. Edmonds, D. A. Griffith, C. J. Rotter, R. B. Ruggeri, D. A. Price, S. Liras, D. J. Craik and D. P. Fairlie, Cyclic Penta- and Hexaleucine Peptides without N-Methylation Are Orally Absorbed, *ACS Med. Chem. Lett.*, 2014, **5**, 1148–1151.

30 Y. Li, W. Li and Z. Xu, Improvement on Permeability of Cyclic Peptide/Peptidomimetic: Backbone N-Methylation as A Useful Tool, *Mar. Drugs*, 2021, **19**, 311.

31 For a study of *N*-Me amide → ester isomerization, and the effect on permeability, see: J. Schwochert, C. Pye, C. Ahlbach, Y. Abdollahian, K. Farley, B. Khunte, C. Limberakis, A. S. Kalgutkar, H. Eng, M. J. Shapiro, A. M. Mathiowetz, D. A. Price, S. Liras and R. S. Lokey, Revisiting N-to-O Acyl Shift for Synthesis of Natural Product-like Cyclic Depsipeptides, *Org. Lett.*, 2014, **16**, 6088–6091.

32 T. Stadelmann, G. Subramanian, S. Menon, C. E. Townsend, R. S. Lokey, M.-O. Ebert and S. Riniker, Connecting the conformational behavior of cyclic octadepsipeptides with their ionophoric property and membrane permeability, *Org. Biomol. Chem.*, 2020, **18**, 7110–7126.

33 (*a*) E. Biron, J. Chatterjee, O. Ovadia, D. Langenegger, J. Brueggen, D. Hoyer, H. A. Schmid, R. Jelinek, C. Gilon, A. Hoffman and H. Kessler, Improving Oral Bioavailability of Peptides by Multiple N-Methylation: Somatostatin Analogues, *Angew. Chem., Int. Ed.*, 2008, **47**, 2595–2599; (*b*) J. Chatterjee, C. Gilon, A. Hoffman and H. Kessler, N-Methylation of Peptides: A New Perspective in Medicinal Chemistry, *Acc. Chem. Res.*, 2008, **41**, 1331–1342; (*c*) T. R. White, C. M. Renzelman, A. C. Rand, T. Rezai, C. M. McEwen, V. M. Gelev, R. A. Turner, R. G. Linington, S. S. F. Leung, A. S. Kalgutkar, J. N. Bauman, Y. Zhang, S. Liras, D. A. Price, A. M. Mathiowetz, M. P. Jacobson and R. S. Lokey, On-resin N-methylation of cyclic peptides for discovery of orally bioavailable scaffolds, *Nat. Chem. Biol.*, 2011, **7**, 810–817.

34 See ESI† for full details.

35 H. Kessler, M. Köck, T. Wein and M. Gehrke, Reinvestigation of the Conformation of Cyclosporin A in Chloroform, *Helv. Chim. Acta*, 1990, **73**, 1818–1832.

36 A. Whitty, M. Zhong, L. Viarengo, D. Beglov, D. R. Hall and S. Vajda, Quantifying the chameleonic properties of macrocycles and other high-molecular-weight drugs, *Drug Discovery Today*, 2016, **21**, 712–717.

37 A consistent protocol and detection method was used for these Caco-2 assays, but this analog was undectable.

38 S. Huh, N. Batistatou, J. Wang, G. J. Saunders, J. A. Kritzer and A. K. Yudin, *Cell penetration of oxadiazole-containing macrocycles*, RSC Chemical Biology, 2024.

39 In most cases, the combination of peak complexity and broadening prevented the application of NMR techniques to examine hydrogen bonding in these compounds. In one case (**1.5**) where titration with DMSO was possible, any differences in hydrogen bonding appeared as an average (see ESI† for experimental details).

40 M. P. Thorpe, D. J. Blackwell, B. C. Knollmann and J. N. Johnston, *J. Med. Chem.*, 2024, **67**, 12205.